New Astronomy 104 (2023) 102084

Contents lists available at ScienceDirect

New Astronomy

journal homepage: www.elsevier.com/locate/newast

Cosmic implications of generalized HDE model in FRW universe

Sarfraz Ali [a,*], Zulaikha Mukhtar [b]

[a] Department of Mathematics, Division of Science and Technology, University of Education, Lahore, Pakistan
[b] Riphah International University, Faisalabad Campus, Pakistan

ARTICLE INFO

Keywords:
Generalized HDE model
EOS
Deceleration parameter
Chern–Simons modified gravity

ABSTRACT

In this study, we investigate a generalized holographic dark energy model within the framework of dynamical Chern–Simons modified gravity theory. By incorporating the Hubble parameter H and its higher order derivatives, we explore the equation of state and its implications for the expansion of the known universe using the Friedmann–Robertson–Walker metric. Our analysis reveals three distinct cases arising from the solutions to the Chern–Simons field equations, which depend on the chosen parameters. In the first two cases, we observe confirmation of the accelerated expansion of the universe, consistent with the predicted range of $-1 < \omega < 0$. However, in the third case, the depicted behavior exhibits a phantom-like nature. It is important to note that irrespective of the case, the generalized holographic dark energy model supports the transition from deceleration to acceleration, aligning well with observational data. Furthermore, our findings establish that the generalized holographic dark energy model endorses the universe's accelerated expansion within the framework of dynamical Chern–Simons modified gravity theory.

1. Introduction

Recent observations indicate that our universe is flat (Spergel et al., 2003; Komatsu et al., 2011), and it is undergoing significant accelerated expansion (Riess et al., 1998; Perlmutter et al., 1999; Knop et al., 2003a). While the presence of a cosmological constant in general relativity (GR) can account for this phase, the magnitude of the cosmological constant remains unexplained by any fundamental theory, despite its agreement with observational data. Consequently, cosmologists have proposed modifications to the gravitational sector or matter distribution in the Einstein–Hilbert action to describe the observed acceleration of the universe.

In light of recent cosmological observations, numerous gravity theories have garnered attention, aiming to elucidate the concepts of late-time accelerated expansion and the gravitational effects on astronomical bodies. It is important to address the unidentified matter and energy sources that fill our universe and are believed to influence gravitational dynamics at cosmological scales, namely dark energy (DE) and dark matter (DM). The challenge in identifying these dark components and distinguishing their effects from modifications of GR on large scales motivates the exploration of innovative gravity theories.

The holographic principle, rooted in the physics of black holes and perturbation theory, incorporates an infrared cutoff of a quantum theory associated with vacuum energy (Susskind, 1995; Witten, 1998). This holographic approach has found wide application in cosmology, particularly in characterizing the era of dark energy, commonly known as the holographic dark energy (HDE) model (Bousso, 2002; Li, 2004; Kumar et al., 2022; Li et al., 2011; Wang et al., 2017; Khurshudyan, 2016; Landim, 2016). It is worth noting that the HDE model differs from other DE models as it is derived from the holographic principle and dimensional analysis rather than introducing an additional term in the Lagrangian. Beyond the era of dark energy, the holographic principle has also been successfully applied to the early inflationary universe. Overall, the combination of observations, theoretical challenges posed by dark energy and dark matter, and the potential offered by the holographic principle has motivated the exploration of modified gravity theories.

By incorporating these concepts into gravitational theories, we aim to gain a deeper understanding of the accelerated expansion of the universe and the dynamics of gravity at both early and late cosmological times. Chakraborty et al. (2021b) and fellows studied the cosmological consequences of Barrow HDE and its thermodynamics under the preview of viscous cosmology. The cosmology of $f(Q)$ gravity and the reconstruction of various associated parameters with different versions of HDE models with generalized cut-offs, where $Q = 6H^2$, is studied in the context of a universe filled with a viscous fluid characterized by a viscous pressure $\Pi = -3H\xi$, where $\xi = \xi_0 + \xi_1 H + \xi_2(\dot{H} + H^2)$ (Chakraborty et al., 2021a). Brevik and Timoshkin (2021) investigated the cosmological models of the late-time universe by incorporating the holographic principle and considering the viscosity properties of the dark fluid utilizing the mathematical formalism

* Corresponding author.
E-mail addresses: sarfaraz.ali@ue.edu.pk (S. Ali), ruhmamukhtar123@gmail.com (Z. Mukhtar).

https://doi.org/10.1016/j.newast.2023.102084
Received 21 March 2023; Received in revised form 13 June 2023; Accepted 14 June 2023
Available online 17 June 2023
1384-1076/

of generalized infrared cutoff holographic dark energy. Karmakar et al. (2020) investigated the reconstruction of $f(R)$ gravity from holographic Ricci dark energy and found a transition from quintessence to phantom era in the absence of bulk viscosity.

The four-dimensional Chern–Simons (CS) modified gravity theory proposed by Jackiw and Pi (2003) is among the most fascinating modeling techniques in reconfigured theories of gravity during the last decades. This theory, which recommends an infringement of parity in Einstein–Hilbert actions, is based on the Pontryagin density. Except if the scalar field is not taken into account as a coupling constant, the density of the Pontryagin term acts as a topological quantity in four-dimensional spacetimes.

In CS theory, Alexander and Yunes (2009) investigated vacuum approximation and exact solutions, as well as Cosmic Baryons asymmetry and inflation. Jawad and Sohail (2015) used modified QCD ghost DE models to investigate the aspects of scalar fields and the possible outcomes of various scalar field models in the framework of dynamical CS (dCS) modified gravity. Sarfraz and fellows (Ali and Amir, 2016; Ali and Saddique, 2021) explored the HDE model and noticed the accelerated expansion of the universe under stringent conditions. Different faces of generalized Holographic dark energy (GHDE) model has been studied in Nojiri et al. (2021, 2019a,b) and Pasqua et al. (2015).

Porfirio and fellows (Porfirio et al., 2016) constituted a relationship for Godel-type spacetime employing four dimensional CS theory for various forms of matter and attributed correlation aspects. Konno et al. (2008) explained rotating black holes in the perspective of the CS theory by admitting a classification of Schwarzschild solutions. Guarrera and Hariton (2007) have discussed a preserved, symmetric energy–momentum pseudo tensor that appears Lorentz invariant in CS theory. The impact of CS theory on the feasible phase shift of de Broglie waves in neutron interferometry was evaluated by Nandi and colleagues (Nandi et al., 2009).

The most common dynamical DE candidates are quintessence (Caldwell et al., 2003) ($-1 < \omega_d < -\frac{1}{3}$), phantom ($\omega_d < -1$) (Guo et al., 2005; Malik et al., 2021), and quintom (Zobnin et al., 2000) etc. The observations lead one to believe an emergent EOS for DE as well (Martin, 2008; Zhuravlev, 2001). As a result, understanding the EOS of DE is one of the most difficult problems in astrophysics (Huterer and Turner, 2001; Huterer and Cooray, 2005; Linder, 2003; Melchiorri et al., 2003) and also in observational cosmology (Knop et al., 2003b; Tegmark et al., 2004).

This article is structured as follows: Section 2 provides the background and functionalism of CS theory, as well as its mathematical model for the FRW metric. In Section 3, the generalized HDE model $\Lambda \sim \rho_{DE} = 3(\mu\frac{\ddot{H}}{H} + \nu\dot{H} + \gamma H^2)$ is investigated. At the end, there is a discussion and analysis of the findings.

2. Formulism of CS theory

This theory is based on the concept of leading-order gravitational parity violation and is one of the possible modifications of GR. This modification was influenced by the cancellation of anomalies in string theory and particle physics. The Einstein–Hilbert action is amended as follows:

$$S = \int_{\upsilon} d^4x\sqrt{-g}\left[\kappa R + \alpha\frac{1}{4}\Theta^{*}RR - \beta\frac{1}{2}(g^{ab}(\nabla_a\Theta)(\nabla_b\Theta) + 2V(\Theta))\right] + \pounds_{mat} \quad (1)$$

where $\pounds_{mat}$ denotes the matter Lagrangian density, $\kappa = \frac{1}{16\pi G}$ (where G is the gravitational constant), and the integrals represent volume integration over the manifold υ. The term ${}^{*}RR$ is technically defined as ${}^{*}RR = R\tilde{R} = {}^{*}R_b^{\;acd}R^b_{\;acd}$, where ${}^{*}R_b^{\;acd} = \frac{1}{2}\epsilon^{cdef}R^a_{\;bef}$ and ϵ^{cdef} is the 4-dimensional Levi-Civita tensor. This term is known as the Pontryagin density.

The parameters α and β are dimensional coupling constants. A natural and commonly used choice for these parameters is $\alpha = 1$, which makes Θ dimensionless, and $\beta = L^2$, suggesting that $\beta \propto \kappa^2$. The choice of coupling constant can have implications for the dimensions of Θ and its physical interpretation.

By perturbing Eq. (1) with respect to g_{ab} and the scalar field Θ (a function of spacetime), a set of CS equations can be derived in the following form:

$$G_{ab} + \alpha C_{ab} = -\frac{1}{2k}(T^m_{ab} + T^\theta_{ab})$$
$$g^{ab}\nabla_a\nabla_b\Theta = -\frac{k\alpha}{4}\;{}^{*}RR, \quad (2)$$

The parameters C_{ab}, G_{ab} and α represent Cotton tensor, Einstein tensor and coupling constant respectively.

$$C^{ab} = -\frac{1}{2\sqrt{-g}}[\upsilon_\sigma\epsilon^{\sigma a\zeta\eta}\nabla_\zeta R^b_\eta + \frac{1}{2}\upsilon_{\sigma\tau}\epsilon^{\sigma b\zeta\eta}R^{\tau a}_{\zeta\eta}] + (a \longleftrightarrow b), \quad (3)$$

The matter part of the field equation Eq. (2) is composed of T^m_{ab} and external scalar field T^Θ_{ab} defined as:

$$T^{(m)}_{ab} = (\rho + P)U_aU_b - Pg_{ab}$$
$$T^{(\theta)}_{ab} = \zeta(\partial_a\Theta)(\partial_b\Theta) - \frac{\zeta}{2}g_{ab}(\partial^\eta\Theta)(\partial_\eta\Theta). \quad (4)$$

In this expression, U, ρ, and p stand for the 4-vector velocity, energy density, and pressure, respectively.

The CS theory is studied in two different domains: the dynamical and non-dynamical formalism. In the non-dynamical case, the CS scalar is a prescribed function, and its conventional evolution corresponds to a differential constraint on the permissible solutions. In the dynamical formulation, the CS term is treated as a dynamical field with an effective stress–energy tensor and an evolution equation. Mathematically, the dynamical framework allows for arbitrary, non-zero constants α and β in Eq. (1) at the level of action. In the non-dynamical framework, however, $\beta = 0$ and α can be arbitrary at the level of action, which means the scalar field does not evolve dynamically but is externally prescribed.

A significant amount of research on CS gravitational modification has been conducted in the non-dynamical framework. In this context, the term "scalar field" Θ is assumed to be a pre-prescribed function of spacetime coordinates. These investigations include the evaluation of both approximate and exact solutions, cosmological and galactic studies, and matter dynamics. However, the non-dynamical theory presents several challenges, including:

(i) Singularities of curvature that appear on the rotational axis of a black hole during rotation;
(ii) The ambiguity regarding the large ensemble of black hole oscillation modes;
(iii) The presence of ghosts, which are typically problematic.

As a result, multiple authors suggest the use of the dynamical CS (dCS) theory with a kinetic term for the scalar field to overcome the aforementioned issues and maintain the self-stability of the theory. The first two issues mentioned above are not present in the dynamical theory, while the third issue does not persist under specific circumstances. Therefore, dynamical CS modified gravity has gained immense popularity.

3. Generalized holographic dark energy model

Einstein's field equations (EFEs) of GR are commonly solved using the FRW metric, which describes an expanding universe that is homogeneous and isotropic. The EFEs are expected to determine the scale factor of the universe as a function of time, while the specific form of the metric arises from the assumption of homogeneity. This model is widely regarded as the standard model of modern cosmology and is also connected to the more advanced Lambda-CDM model. The line element is given by:

$$ds^2 = dt^2 - \Re^2(t)[\frac{1}{1-kr^2}dr^2 + r^2(d\theta^2 + sin^2\theta d\phi^2)]. \quad (5)$$

where $\mathfrak{R}(t)$ denotes the scale factor that describes the expansion of the Universe, (r, θ, ϕ) represent the spatial coordinates. The curvature of space is indicated by the non-zero components of the Einstein tensor, which can be listed as follows:

$$\begin{aligned} G_{00} &\equiv \frac{3}{\mathfrak{R}^2}(\dot{\mathfrak{R}}^2+\kappa), \\ G_{11} &\equiv -\left(\frac{2\mathfrak{R}\ddot{\mathfrak{R}}+\dot{\mathfrak{R}}^2+\kappa}{1-\kappa r^2}\right), \\ G_{22} &\equiv -r^2(\kappa+\dot{\mathfrak{R}}^2+2\mathfrak{R}\ddot{\mathfrak{R}}), \\ G_{33} &\equiv -r^2\sin^2\theta(\kappa+\dot{\mathfrak{R}}^2+2\mathfrak{R}\ddot{\mathfrak{R}}). \end{aligned} \tag{6}$$

A flat universe is described by the conventional Friedmann equation, which is obtained by setting $8\pi G$ (appearing in the Einstein equations) to unity for simplicity.

$$H^2 = \frac{1}{3}\rho, \tag{7}$$

According to the holographic principle, the degrees of freedom of a system are related to its surface area rather than its volume. This principle has been extensively studied as an effective approach to address the mystery of dark energy (DE) and has garnered significant interest in recent years. In particular, the holographic dark energy (HDE) model connects the infrared and ultraviolet cutoffs to the energy density of quantum fields in vacuum, serving as a candidate for DE. Within this framework, a generalized holographic dark energy (GHDE) model can be expressed as follows:

$$\rho_{DE} = 3(\mu\frac{\ddot{H}}{H}+\nu\dot{H}+\gamma H^2). \tag{8}$$

In the given equation, H represents the Hubble parameter and $\dot{H}$ denotes its derivative. The dimensionless constants μ, ν, and γ are introduced in the expression. The motivation behind choosing this particular form of the density of dark energy (DE) in Eq. (8) is to rewrite the Friedmann equation (Eq. (5)) as a second-order differential equation (see Eq. (9) below), which enables us to analyze the general solutions. This simplifies the investigation of the model's properties in subsequent calculations. To ensure the dimensions of the terms in Eq. (2) are consistent, we include the inverse of the Hubble parameter, H^{-1}, in the first term of the DE density. Additionally, when $\mu = 0$, this model reduces to the modified Ricci DE model (Granda and Oliveros, 2009, 2008; Ali and Amir, 2019), which has been studied in the context of general relativity and other modified theories (Wang et al., 2017; Amir and Ali, 2015; Jahromi et al., 2018; Younas et al., 2019; Moradpour et al., 2018; Ali et al., 2021). In summary, the motivations behind the development of generalized HDE models include addressing the cosmic coincidence problem, accommodating time variation of dark energy, incorporating interactions with matter, and improving consistency with observational data from various cosmological probes. These models aim to provide a more comprehensive and accurate understanding of the nature of dark energy in the universe.

Let us change the variable $x = \ln\mathfrak{R}$, which can be further evaluated as $\dot{H} = \frac{d}{dt}H$ and $\dot{H} = \frac{d}{dx}\cdot\frac{dx}{dt}H$. Thus, $\dot{H} = \frac{1}{2}\frac{dH^2}{dx}$. Using these substitutions in Eq. (8):

$$\rho_{DE} = 3\left(\frac{\mu}{2}\frac{d^2H^2}{dx^2}+\frac{\nu}{2}\frac{dH^2}{dx}+\gamma H^2\right). \tag{9}$$

The energy conservation equation is given by:

$$\dot{\rho}_m + 3H(\rho_m + p_m) = 0. \tag{10}$$

In the absence of pressure, substituting $p_m = 0$ in Eq. (10), it becomes:

$$\rho_m = \rho_{m_0}e^{-3x}. \tag{11}$$

Using Eq. (4), one can explore the density parameter for the scalar field Θ:

$$\rho_\theta = \frac{1}{6}\dot{\Theta}. \tag{12}$$

Since Θ is taken as a function of spacetime coordinates, we consider it only depends on the time coordinate.

$$\ddot{\Theta} + \frac{3\dot{\mathfrak{R}}}{\mathfrak{R}}\dot{\Theta} = 0, \tag{13}$$

Solving the differential Eq. (13) we get $\dot{\Theta} = c_2\mathfrak{R}^{-3}$ and suppose $\frac{c_2}{6} = \rho_{\Theta_0}$ and $x = \ln\mathfrak{R}$, one concluded that

$$\rho_\Theta = \rho_{\Theta_0}e^{-6x}, \tag{14}$$

Making use of Eqs. (9), (11) and Eq. (14) in Eq. (7), authors explored that

$$H^2 = \frac{\mu}{2}\frac{d^2H^2}{dx^2}+\frac{\nu}{2}\frac{dH^2}{dx}+\gamma H^2+\rho_{m_0}e^{-3x}+\rho_{\Theta_0}e^{-6x}. \tag{15}$$

Normalizing Eq. (15) using $\hbar = \frac{H}{H_0}$, where H_0 indicates the Hubble parameter at the initial value of $x = 0$, and further making substitutions $\Omega_{\Theta_0} = \frac{\rho_{\Theta_0}}{3H_0^2}$ and $\Omega_{m_0} = \frac{\rho_{m_0}}{3H_0^2}$, we arrive at

$$\frac{\mu}{2}\frac{d^2\hbar^2}{dx^2}+\frac{\nu}{2}\frac{d\hbar^2}{dx}+(\gamma-1)\hbar^2+\Omega_{m_0}e^{-3x}+\Omega_{\Theta_0}e^{-6x} = 0. \tag{16}$$

For the analytic solution of the differential equation Eq. (16) using the substitution $\hbar^2 = y$, the solution is given by

$$\mu\frac{d^2y}{dx^2}+\nu\frac{dy}{dx}+2(\gamma-1)y = -2(\Omega_{m_0}e^{-3x}+\Omega_{\theta 0}e^{-6x}). \tag{17}$$

Now, let us explore the complementary part of Eq. (17) by considering the solution for $(C.F)$ (complementary function) using the substitution $y = e^{zx}$. Differentiating with respect to x, we have $\frac{dy}{dx} = ze^{zx}$, and differentiating again gives $\frac{d^2y}{dx^2} = z^2e^{zx}$.

Substituting these expressions into Eq. (17), we have:

$$[\mu z^2+\nu z+2(\gamma-1)]e^{zx} = 0 \tag{18}$$

Since $e^{zx} \neq 0$, we can conclude that:

$$\mu z^2+\nu z+2(\gamma-1) = 0 \tag{19}$$

To obtain real roots, we can use basic algebraic formulations. The complementary solution is then given by:

$$y_c = \alpha_1 e^{\frac{-\nu-\sqrt{\nu^2-8\mu(\gamma-1)}}{2\mu}x}+\alpha_2 e^{\frac{-\nu+\sqrt{\nu^2-8\mu(\gamma-1)}}{2\mu}x}. \tag{20}$$

Here, α_1 and α_2 are constants of integration, which can be determined based on the initial conditions. The particular solution of Eq. (17) is given by:

$$y_p = \frac{2\Omega_{m_0}e^{-3x}}{(2-9\mu+3\nu-2\gamma)}+\frac{\Omega_{\Theta_0}e^{-6x}}{1-18\mu+3\nu-\gamma}, \tag{21}$$

The net solution is then given by $y = y_c + y_p$. By using backward substitution, we arrive at

$$\begin{aligned} y = {} & \Omega_{m_0}e^{-3x}+\Omega_{\Theta_0}e^{-6x} \\ & + \alpha_1 e^{\frac{-\nu-\sqrt{\nu^2-8\mu(\gamma-1)}}{2\mu}x}+\alpha_2 e^{\frac{-\nu+\sqrt{\nu^2-8\mu(\gamma-1)}}{2\mu}x} \\ & + \frac{(9\mu-3\nu+2\gamma)}{(2-9\mu+3\nu-2\gamma)}\Omega_{m_0}e^{-3x}+\frac{(18\mu-3\nu+\gamma)}{1-18\mu+3\nu-\gamma}\Omega_{\Theta_0}e^{-6x}. \end{aligned} \tag{22}$$

Again using backward substitution $y = \hbar^2$ in Eq. (22)

$$\begin{aligned} \hbar^2 = {} & \Omega_{m_0}e^{-3x}+\Omega_{\Theta_0}e^{-6x} \\ & + \alpha_1 e^{\frac{-\nu-\sqrt{\nu^2-8\mu(\gamma-1)}}{2\mu}x}+\alpha_2 e^{\frac{-\nu+\sqrt{\nu^2-8\mu(\gamma-1)}}{2\mu}x} \\ & + \frac{(9\mu-3\nu+2\gamma)}{(2-9\mu+3\nu-2\gamma)}\Omega_{m_0}e^{-3x}+\frac{(18\mu-3\nu+\gamma)}{1-18\mu+3\nu-\gamma}\Omega_{\Theta_0}e^{-6x}. \end{aligned} \tag{23}$$

By using the initial conditions $x = 0$ and $\hbar^2 = 1$, we can evaluate the expression in terms of α_1 and α_2 from Eq. (23):

$$1 = \alpha_1+\alpha_2+\frac{1}{1-18\mu+3\nu-\gamma}\Omega_{m_0}+\frac{2}{2-9\mu+3\nu_2\gamma}\Omega_{\Theta_0}, \tag{24}$$

From Eq. (24), we deduce that it is impossible to precisely determine the integration constants α_1 and α_2. In other words, there is a free

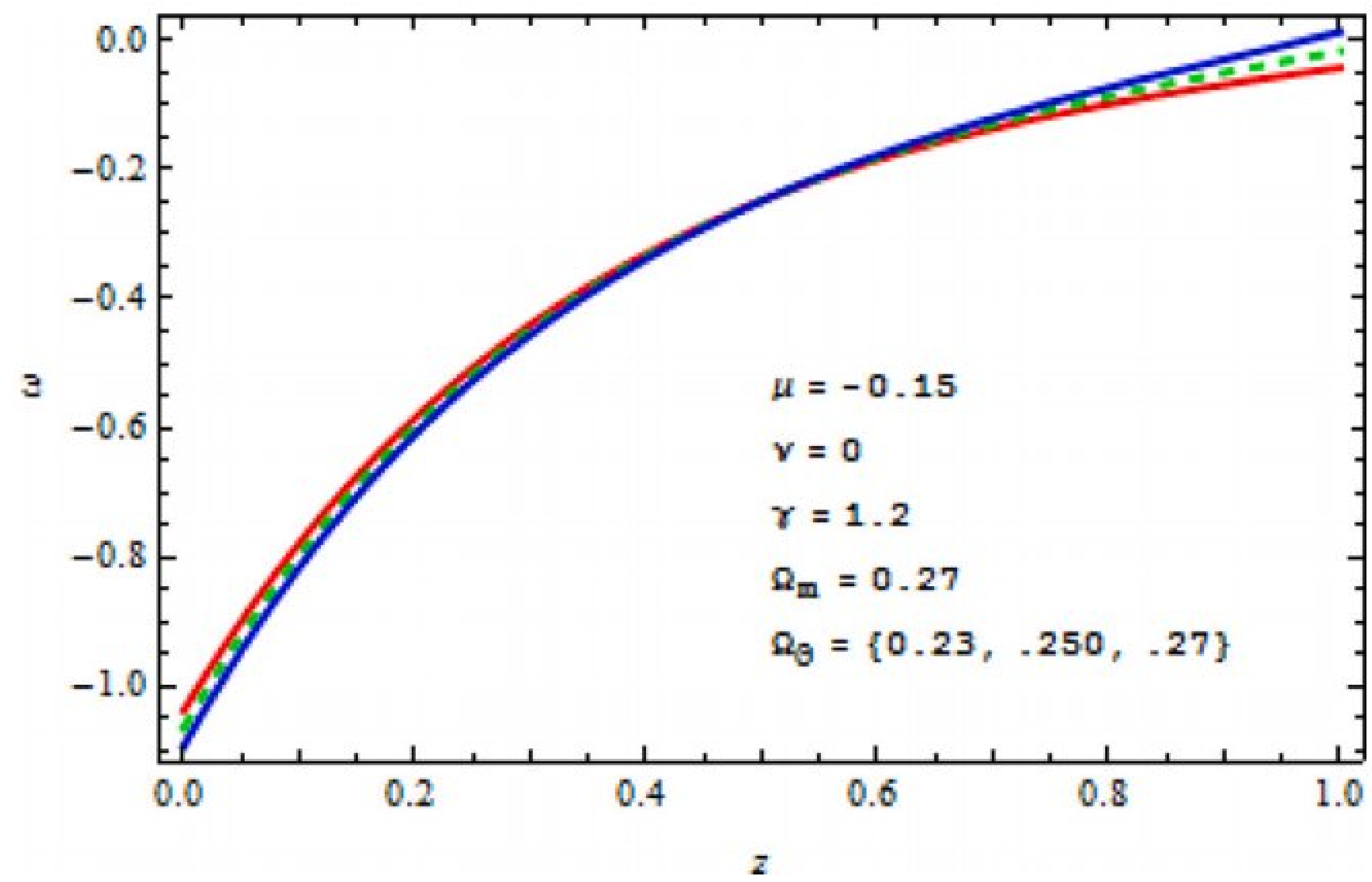

Fig. 1.

integration constant between α_1 and α_2. For simplicity, we can consider scenarios where $\alpha_1 = 0$, $\alpha_2 = 0$, or $\alpha_1 = \alpha_2$. After that, we can examine the characteristics of the dark energy model given by Eq. (8) and address the age problem.

4. Case I

Let us repeat the procedure of normalizing Eq. (7) by considering the equation: $\frac{H^2}{H_0^2} = \hbar^2 = \Omega_{de} + \Omega_{m_0} e^{-3x} + \Omega_{\Theta_0} e^{-6x}$. Now, we equate this with Eq. (23) by substituting $\alpha_2 = 0$. This allows us to obtain the expressions for the density and pressure of dark energy, which can be shown as

$$\Omega_{de} = \alpha_1 e^{\frac{-\nu-\sqrt{\nu^2-8\mu(\gamma-1)}}{2\mu}x} + \frac{9\mu - 3\nu + 2\gamma}{(2 - 9\mu + 3\nu - 2\gamma)}\Omega_{m_0} e^{-3x} + \frac{18\mu - 3\nu + \gamma}{1 - 18\mu + 3\nu - 2\gamma}\Omega_{\Theta_0} e^{-6x}. \tag{25}$$

or

$$\rho_{DE} = H_0^2[\alpha_1 e^{\frac{-\nu-\sqrt{8\mu(\gamma-1)}}{2\mu}x} + \frac{9\mu - 3\nu + 2\gamma}{(2 - 9\mu + 3\nu - 2\gamma)}\Omega_{m_0} e^{-3x} + \frac{18\mu - 3\nu + \gamma}{1 - 18\mu + 3\nu - 2\gamma}\Omega_{\Theta_0} e^{-6x}], \tag{26}$$

and the pressure in terms of density parameter is $P_{DE} = -\rho_{DE} - \frac{1}{3}\frac{d\rho_{DE}}{dx}$

$$P_{DE} = -H_0^2[\frac{6\mu - \nu + \sqrt{\nu^2 - 8\mu(\gamma - 1)}}{6\mu}\alpha_1 e^{\frac{-\nu-\sqrt{\nu^2-8\mu(\gamma-1)}}{2\mu}x} - \frac{(18\mu - 3\nu + \gamma)}{1 - 18\mu + 3\nu - \gamma}\Omega_{\Theta_0} e^{-6x}]. \tag{27}$$

To obtain the value of α_1, suppose that $\alpha_2 = 0$ in Eq. (24). Then, we have:

$$\alpha_1 = \frac{(2 - 9\mu + 3\nu - 2\gamma) - 2\Omega_{m0}}{6\mu - \nu + \sqrt{\nu^2 - 8\mu(\gamma - 1)}} - \frac{\Omega_{\Theta_0}}{1 - 18\mu + 3\nu - \gamma}. \tag{28}$$

The equation of state (EOS) is commonly used to understand the dynamics and structure of astronomical systems. It represents the relationship between the total energy density of cosmic matter and the total pressure in the cosmos. Another important parameter used in cosmology is the deceleration parameter, which is a dimensionless quantity that characterizes the cosmological acceleration of the universe. The EOS is defined as $\omega = \frac{P_{DE}}{\rho_{DE}}$. By substituting the respective values from Eqs. (26) and (27), the result can be expressed as

$$\omega_1 = -\frac{\Psi_1\left[(1-\Psi_3)(\Psi_1 - 2\Omega_{m_0})e^{\frac{(\Psi_1-6\mu)x}{2\mu}} - \Omega_{\Theta_0}[e^{\frac{(\Psi_1-6\mu)x}{2\mu}} + 6\mu\Psi_3 e^{-3x}]\right]}{6\mu\left[(1-\Psi_3)(2-\Psi_2)(\Psi_1 - 2\Omega_{m_0})\Omega_{m0}e^{\frac{(\Psi_1-6\mu)x}{2\mu}} - \Psi_1\Omega_{\Theta_0}(e^{\frac{(\Psi_1-6\mu)x}{2\mu}} - \Psi_3 e^{-3x})\right]}. \tag{29}$$

where

$$\Psi_1 = 6\mu - \nu + \sqrt{\nu^2 - 8\mu(\gamma - 1)},$$
$$\Psi_2 = (2 - 9\mu + 3\nu - 2\gamma),$$
$$\Psi_3 = 1 - 18\mu + 3\nu - \gamma. \tag{30}$$

The deceleration parameter q in terms of the equation of state parameter ω is given mathematically as: $q = \frac{1}{2}(1+3\omega)$. This relationship allows us to determine the deceleration or acceleration of the universe based on the value of the equation of state parameter.

$$q = \frac{1}{2}(1 + 3\omega) \tag{31}$$

Using Eq. (29) in Eq. (31), we can derive the expression for the deceleration parameter q as follows:

$$q_1 = \frac{1}{2} - \frac{\Psi_1\left[-e^{\frac{(\Psi_1-6\mu)x}{2\mu}}(-1+\Psi_3)(\Psi_1 - 2\Omega_{m_0}) - \Omega_{\Theta_0}[e^{\frac{(\Psi_1-6\mu)x}{2\mu}} + 6\mu\Psi_3 e^{-3x}]\right]}{4\mu\left[e^{\frac{(\Psi_1-6\mu)x}{2\mu}}(-2+\Psi_2)(-1-\Psi_3)(\Psi_1 - 2\Omega_{m_0})\Omega_{m0} - \Psi_1\Omega_{\Theta_0}(e^{\frac{(\Psi_1-6\mu)x}{2\mu}} + \Psi_3 e^{-3x})\right]}. \tag{32}$$

To comprehend the cosmic evolution of the equation of state parameter ω and the deceleration parameter q, graphs can be plotted based on the equations provided in Eqs. (29) and (32). These equations indicate that ω and q are functions of x and depend on various cosmological variables.

By plotting these graphs, one can visualize the behavior of ω and q as the universe evolves. This can provide insights into the acceleration or deceleration of the universe, as well as the nature of the dark energy component.

The given limitations on the parameters μ, ν, γ, and Ω_{m_0}, along with the specific values of Ω_{θ_0} shown in Fig. 1, have implications for the behavior of the equation of state (EOS). In cosmology, the EOS is used to describe different eras in which specific components dominate the universe.

For example, EOS values of $\omega = 0$, $\frac{1}{3}$, and 1 correspond to eras dominated by dust, radiation, and stiff fluids, respectively. On the other hand, values of $-\frac{1}{3}$, -1, and $\omega < -1$ correspond to the quintessence dark energy, ΛCDM (cosmological constant), and phantom ages, respectively. Based on the graph in Fig. 1, it is evident that the universe is currently undergoing accelerated expansion, indicating the influence of dark energy. The current GHDE model predicts a range of EOS values $\omega_1 \in (-1.22, -1)$ for the specified parameter values. It is noteworthy that this range is consistent with recent observational constraints obtained from data such as Planck+WP+Union 2.1

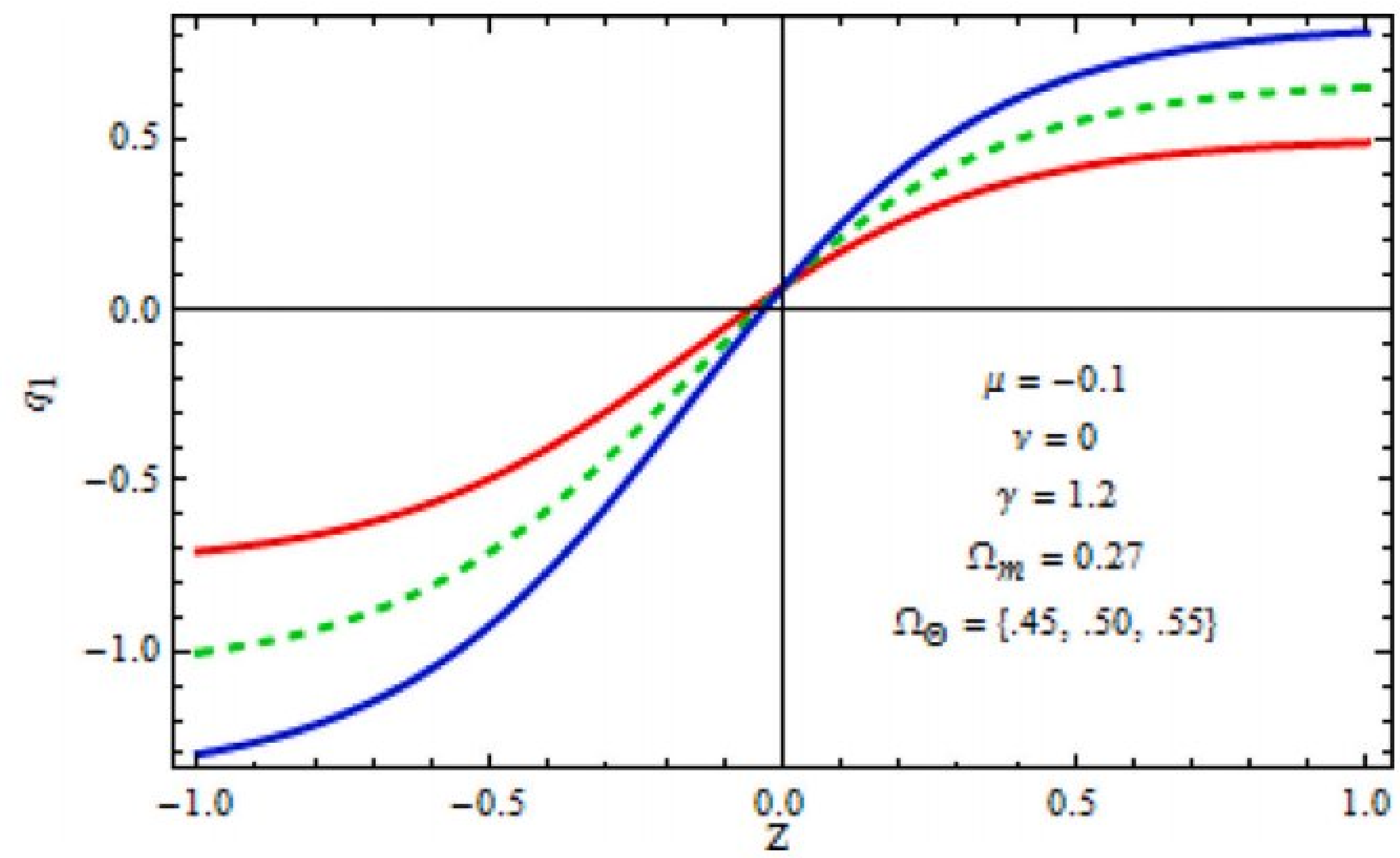

Fig. 2.

($-1.26 < \omega < -0.92$), Planck+WP+BAO ($-1.38 < \omega < -0.89$), and WMAP+eCMB+BAO+H0 ($-1.162 < \omega < -0.983$) measurements (Refs. Aghanim et al. (2020), Hossienkhani et al. (2021), Shekh (2021), Telali and Saridakis (2022), Shaikh (2022) and Nojiri and Odintsov (2017)). These observations support the compatibility of the GHDE model with the current observational constraints and suggest that the model provides a reasonable description of the accelerated expansion phase of the universe.

Fig. 2 depicts the cosmic evolution of the deceleration parameter q. It shows an accelerated phase for $q > 0$ at high redshift and a decelerated phase for $q < 0$ at $x = 0$. This graphical representation supports the transition from deceleration to acceleration, which is also anticipated in Refs. Ma (2008), Daly et al. (2008), Perlmutter et al. (1999), Amir and Ali (2016) and Wang et al. (2017).

The behavior of the deceleration parameter is observed to be similar in all three cases. Notably, the GHDE model supports the transition from deceleration to acceleration, which is consistent with observational data. This is a significant result, as it aligns with the observed acceleration of the universe and provides further support for the validity of the GHDE model.

5. Case-II

Let us suppose $\alpha_1 = 0$ while α_2 is nonzero and working on the same lines as followed in Case-I, the energy density ρ_{DE} is evaluated on equating Eqs. (23) and (24),

$$\rho_{DE} = H_0^2[\alpha_2 e^{\frac{-\nu+\sqrt{\nu^2-8\mu(\gamma-1)}}{2\mu}x} + \frac{9\mu-3\nu+2\gamma}{(2-9\mu+3\nu-2\gamma)}\Omega_{m_0}e^{-3x} + \frac{18\mu-3\nu+\gamma}{1-18\mu+3\nu-\gamma}\Omega_{\Theta_0}e^{-6x}]. \tag{33}$$

The expression for pressure of DE model is obtained as

$$P_{DE} = H_0^2[\frac{-\nu+\sqrt{\nu^2-8\mu(\gamma-1)}}{6\mu}\alpha_2 e^{\frac{-\nu+\sqrt{\nu^2-8\mu(\gamma-1)}}{2\mu}x} - \frac{18\mu-3\nu+\gamma}{1-18\mu+3\nu-\gamma}\Omega_{\Theta_0}e^{-3x}]. \tag{34}$$

Using Eq. (22) one can evaluate

$$\alpha_2 = \frac{(2-9\mu+3\nu-2\gamma)-2\Omega_{m_0}}{(2-9\mu+3\nu-2\gamma)} - \frac{\Omega_{\Theta_0}}{1-18\mu+3\nu-\gamma}. \tag{35}$$

Making use of Eqs. (33), (34) and (35), we evaluated ω_2 such that

$$\omega_2 = -\frac{\Psi_1\Psi_3(\Psi_2-2\Omega_{m_0})e^{-3x} - (\Psi_2)\Omega_{\Theta_0}[(\Psi_1)e^{-3x} + (1-\Psi_3)e^{\frac{(\Psi_1-6\mu)x}{2\mu}}]}{6\mu\left[\Psi_3(2-\Psi_2)\Omega_{m_0} - (\Psi_2(1-2\Psi_3)e^{\frac{(\Psi_1-6\mu)x}{2\mu}} + (\Psi_2-2\Omega_{m_0}) - \Psi_2\Omega_{\Theta_0})e^{-3x}\right]}. \tag{36}$$

Further, the expression for deceleration parameter q_2 in this case is represented as

$$q_2 = \frac{1}{2}\left[1 + \frac{e^{-3x}(\Psi_1(-2\Psi_3\Omega_{m_0} + \Psi_2(\Psi_3 - \Omega_{\Theta_0})) + e^{\frac{(\Psi_1-6\mu)x}{2\mu}}\Psi_2(-1+\Psi_3)\Omega_{\Theta_0})}{2\mu\left((-2+\Psi_2)\Psi_3\Omega_{m_0} + \Psi_2 e^{-3x}(e^{\frac{(\Psi_1-6\mu)x}{2\mu}}(1-2\Psi_3)(\Psi_2-2\Omega_{m_0}) - \Omega_{\Theta_0})\right)}\right]. \tag{37}$$

To study the effect of EOS and q given in Eqs. (36) and (37), the graphs are plotted here.

Let us impose certain limitations on the parameters μ, ν, γ, Ω_{m_0}, and Ω_{θ_0} mentioned in Figs. 3 and 4. Since the equation of state (EOS) predicts an accelerated expansion phase, it is graphically evident that the universe is being influenced by dark energy (DE). In the second case, the GHDE model also explicitly predicts the value of EoS ω_2 to be within the range of (-1.22, -1) for the specified parameter values. This range is consistent with recent observational constraints obtained from Planck+Union 2.1+BAO and WMAP+eCMB+BAO+H0 measurements (Aghanim et al., 2020; Hossienkhani et al., 2021; Shekh, 2021; Telali and Saridakis, 2022; Shaikh, 2022; Nojiri and Odintsov, 2017). The behavior of the deceleration parameter has been found to be consistent across all three scenarios. It is worth noting that the GHDE model supports the transition from deceleration to acceleration, which is in accordance with experimental observations (Riess et al., 1998; Perlmutter et al., 1999; Ma, 2008; Daly et al., 2008; Perlmutter et al., 1999; Amir and Ali, 2016).

6. Case III

Now, we consider $\alpha_1 = \alpha_2$ in Eq. (22) turned out to be

$$\alpha_1 = \alpha_2 = \frac{(2-9\mu+3\nu-2\gamma)-2\Omega_{m_0}}{2(2-9\mu+3\nu-2\gamma)} - \frac{\Omega_{\Theta_0}}{2(1-18\mu+3\nu-\gamma)}. \tag{38}$$

Working on same lines the ρ_{DE} and P_{DE} are calculated as

$$\rho_{DE} = H_0^2\left[\alpha_1(e^{-\frac{\nu+\sqrt{\nu^2-8\mu(\gamma-1)}}{2\mu}x} + e^{-\frac{\nu-\sqrt{\nu^2-8\mu(\gamma-1)}}{2\mu}x}) + \frac{9\mu-3\nu+2\gamma}{2-9\mu+3\nu-2\gamma}\Omega_{m_0}e^{-3x} + \frac{18\mu-3\nu+\gamma}{1-18\mu+3\nu-\gamma}\Omega_{\Theta_0}e^{-6x}\right]. \tag{39}$$

and

$$P_{DE} = H_0^2\left[-\frac{(18\mu-3\nu+\gamma)}{(1-18\mu+3\nu-\gamma)}\Omega_{\Theta_0}e^{-6x} + \frac{\alpha_1}{6\mu} \times [(\nu+\sqrt{\nu^2-8\mu(\gamma-1)}-6\mu) \times e^{-\frac{\nu+\sqrt{\nu^2-8\mu(\gamma-1)}}{2\mu}x} + (\nu-\sqrt{\nu^2-8\mu(\gamma-1)}-6\mu) \times e^{-\frac{\nu-\sqrt{\nu^2-8\mu(\gamma-1)}}{2\mu}x}]\right]. \tag{40}$$

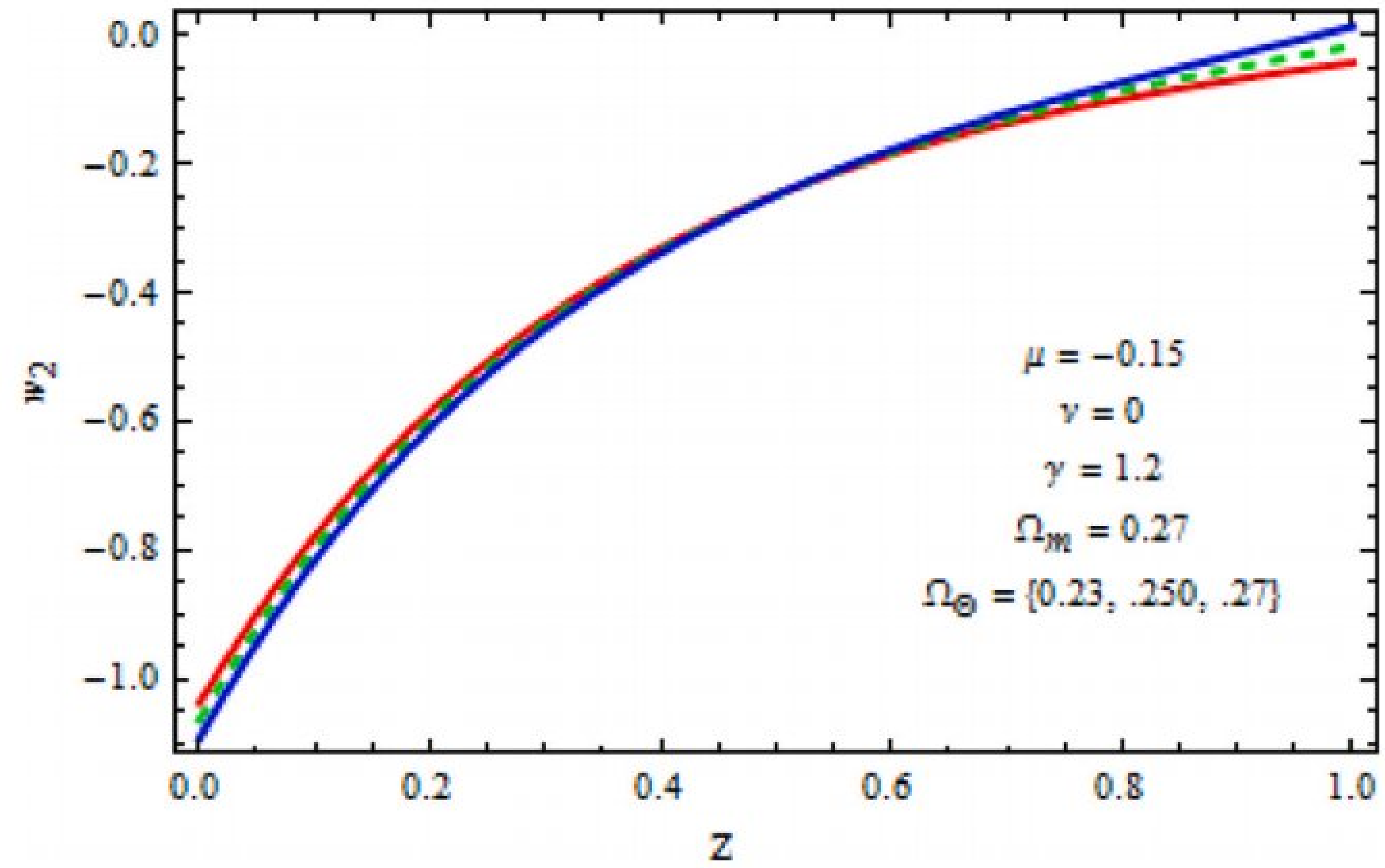

Fig. 3.

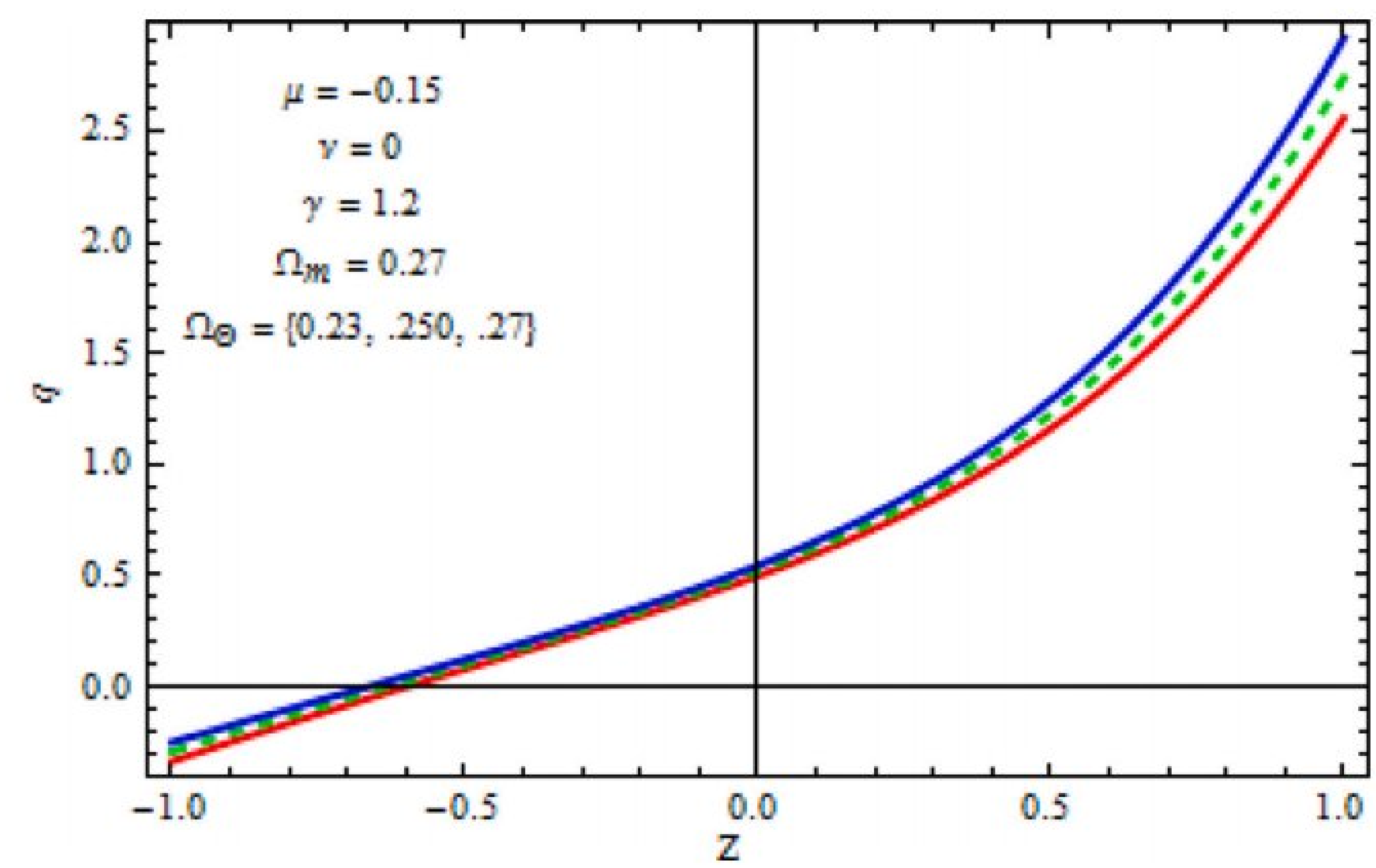

Fig. 4.

and EOS is evaluated as

$$w_3 = -\frac{\Psi_1 \Psi_M e^{\frac{\Psi_1 - 6\mu}{2\mu}x} - 12\mu \Psi_2 (\Psi_3 - 1)\Omega_{\Theta 0} e^{-6x}}{6\mu\left(\Psi_M e^{\frac{\Psi_1 - 6\mu}{2\mu}x} + 2\Psi_2(\Psi_3 - 1)\Omega_{\Theta 0} e^{-6x} + 2(2 - \Psi_2)\Psi_3 \Omega_{m0} e^{-3x}\right)}. \tag{41}$$

where

$$\begin{aligned} \Psi_1 &= 6\mu - \nu + \sqrt{\nu^2 - 8\mu(\gamma - 1)}, \\ \Psi_2 &= (2 - 9\mu + 3\nu - 2\gamma), \\ \Psi_3 &= 1 - 18\mu + 3\nu - \gamma, \\ \Psi_M &= [\Psi_1 \Psi_3 - 2\Psi_3 \Omega_{m0} - \Psi_2 \Omega_{\Theta 0}] \end{aligned} \tag{42}$$

$$q_3 = \frac{1}{2}\left[1 - \frac{\Psi_1 \Psi_M e^{\frac{\Psi_1 - 6\mu}{2\mu}x} - 12\mu \Psi_2 (\Psi_3 - 1)\Omega_{\Theta 0} e^{-6x}}{2\mu\left(\Psi_M e^{\frac{\Psi_1 - 6\mu}{2\mu}x} + 2\Psi_2(\Psi_3 - 1)\Omega_{\Theta 0} e^{-6x} + 2(2 - \Psi_2)\Psi_3 \Omega_{m0} e^{-3x}\right)}\right]. \tag{43}$$

For graphical study of EOS and deceleration parameter given in Eq. (41) and (43), we plotted graphs in Figs. 5 and 6 .

Fig. 5 indicates a decreasing trend for the chosen parameters μ, ν, γ, Ω_{m_0}, and Ω_{Θ_0}, which leads to phantom-like eras. The current values of the equation of state (EoS) parameter for the present model predict $\omega_3 \in (-\frac{1}{3}, -0.2)$ for the considered parameter values. However, it is important to note that this range is not consistent with the recent observational constraints obtained from Planck+WP+Union 2.1 ($-1.26 < \omega < -0.92$), Planck+WP+BAO ($-1.38 < \omega < -0.89$), and WMAP+eCMB+BAO+H0 ($-1.162 < \omega < -0.983$) measurements (Aghanim et al., 2020; Hossienkhani et al., 2021; Nojiri et al., 2021; Bhatti et al., 2023; Shekh, 2021; Telali and Saridakis, 2022; Shaikh, 2022; Nojiri and Odintsov, 2017).

In terms of the evolution of the deceleration parameter as a function of x, for the same values of the free parameters as shown in Fig. 6, it is noteworthy that the transition from acceleration ($q < 0$) to deceleration ($q > 0$) occurs at $x = -0.5$, which is similar to what was found in Ma (2008) and Mamon (2020).

7. Summary and discussion

Multiple studies, such as Type Ia supernovae (SN) (Spergel et al., 2003), the cosmic microwave background (CMB) (Komatsu et al., 2011), and large-scale structures (Riess et al., 1998), have conclusively demonstrated that the universe is undergoing an accelerating expansion. The late-time cosmic acceleration poses challenges to our understanding of fundamental theories of gravity. According to Einstein's general relativity predictions, the universe is filled with a mysterious substance called "dark energy", which is believed to be

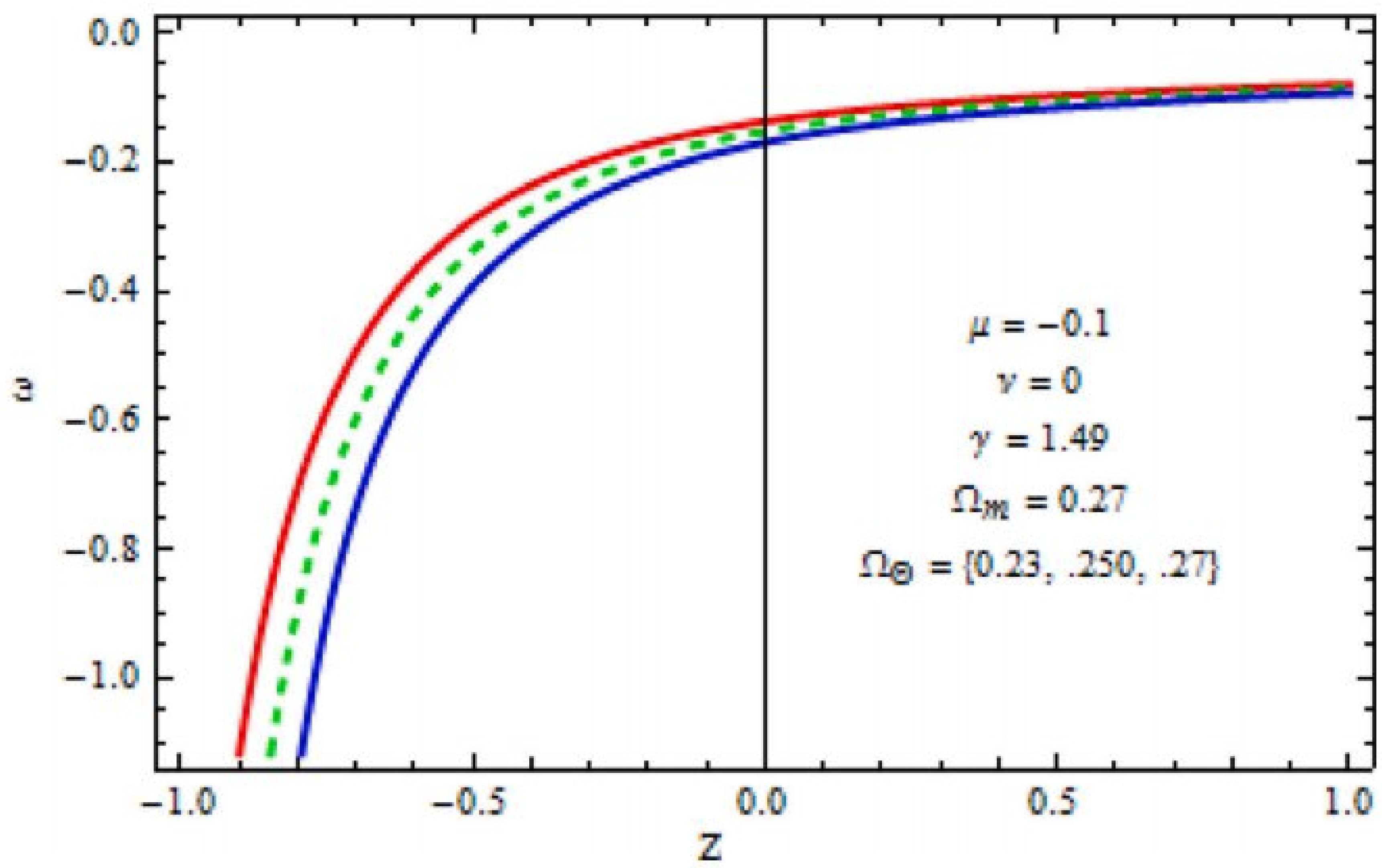

Fig. 5.

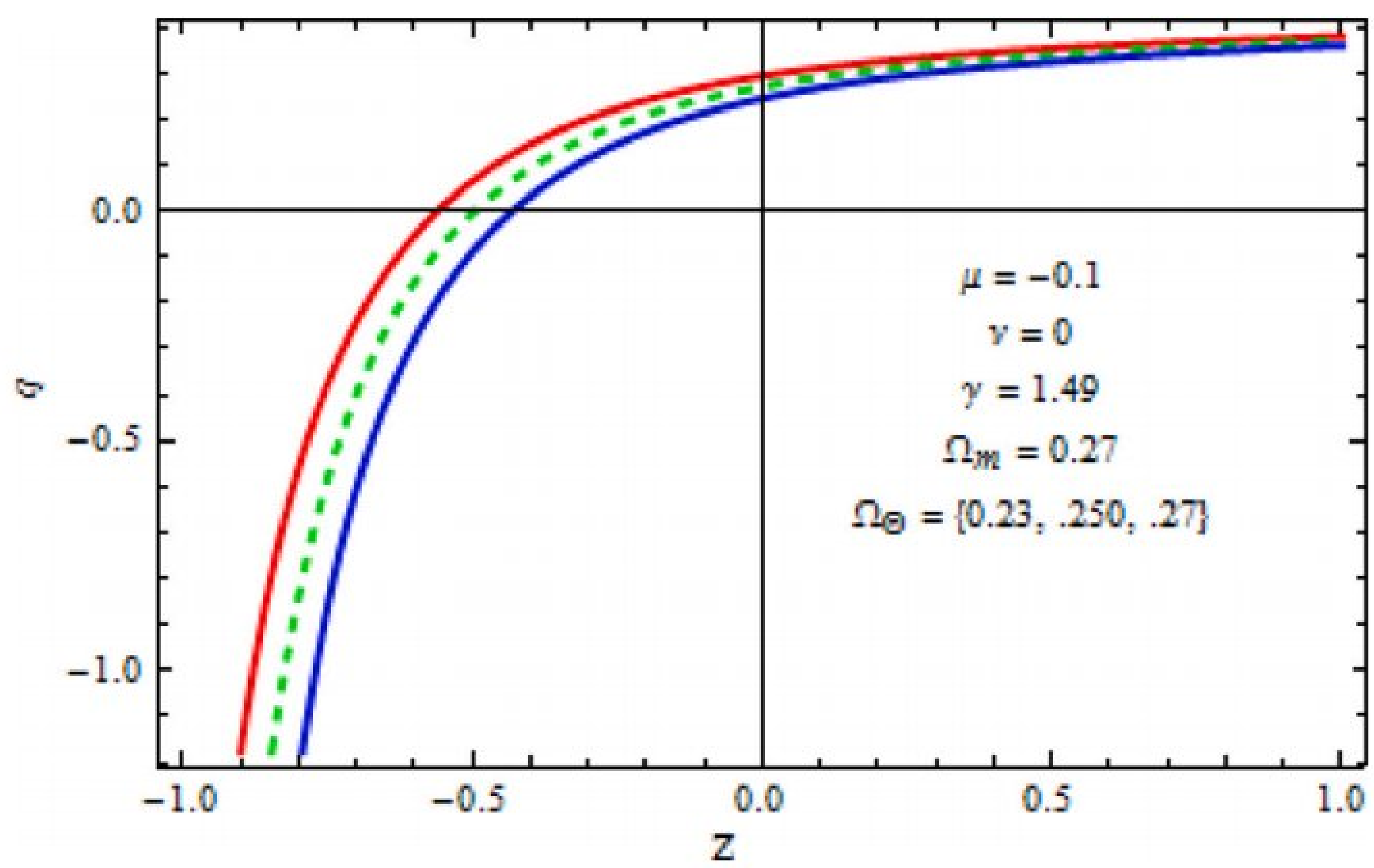

Fig. 6.

responsible for this expansion. In the context of dCS modified gravity theory, this paper investigates a GHDE model that incorporates the Hubble parameter H and its higher-order derivatives. We analyze the expansion of the universe by examining the energy density, pressure, deceleration parameter, and equation of state (EOS), considering the Friedmann–Robertson–Walker (FRW) metric. Our findings indicate that in the first two cases, $-1 < \omega < 0$ predicts the accelerated expansion of the universe under the influence of dark energy, while in the third case, a phantom-like behavior is observed.

Fig. 2 illustrates an accelerated phase with $q > 0$ at high redshift and a decelerated phase with $q < 0$ at $x = 0$. Our graphical representation supports the transition from deceleration to acceleration, which is also anticipated in Amir and Ali (2015), Ma (2008), Daly et al. (2008), Perlmutter et al. (1999), Amir and Ali (2016), and Wang et al. (2017). It is noteworthy that the behavior of the deceleration parameter is similar in all three cases. Importantly, the GHDE model supports the transition from deceleration to acceleration, which aligns with experimental observations (Riess et al., 1998; Perlmutter et al., 1999; Ma, 2008; Daly et al., 2008; Perlmutter et al., 1999; Amir and Ali, 2016).

Additionally, it is worth noting that in case III, the acceleration $q < 0$ transitions to deceleration $q > 0$ at $x = -0.5$, which is consistent with the findings in Ma (2008) and Mamon (2020). It is also emphasized that the parameter values of μ, ν, and γ, along with the density parameters Ω_m and Ω_Θ, have a significant impact on the behavior of dark energy and the expansion history of the universe. In conclusion, the GHDE model in the framework of dynamical CS modified gravity theory supports the universe's accelerated expansion.

Declaration of competing interest

The authors declare that they have no known competing financial interests or personal relationships that could have appeared to influence the work reported in this paper.

Data availability

Data will be made available on request

Funding information

This study is not funded by any organization.

References

Aghanim, N., et al., 2020. Planck 2018 results. Astron. Astrophys. 641, A6, erratum:; 2021. Astron. Astrophys. 652, C4.
Alexander, S., Yunes, N., 2009. Chern–Simons modified general relativity. Phy. Rep. 480, 1–55.

Ali, S., Amir, M.J., 2016. A study of holographic dark energy models in Chern-Simon modified gravity. Internat. J. Theoret. Phys. 55, 5095.
Ali, S., Amir, M.J., 2019. Cosmological analysis of modified holographic Ricci dark energy in Chern–Simons modified gravity. Adv. High Energy Phys. 2019, 3709472. http://dx.doi.org/10.1155/2019/3709472, 9 pages.
Ali, S., Saddique, M., 2021. Time dependent gravitational constant in Chern–Simons modified gravity. Iran. J. Phys. Res. 21, 3.
Ali, S., Waheed, M.H., Asjad, M.I., Khan, K.A., Sitthiwirattham. T. and, C., 2021. The Sharma–Mittal model's implications on FRW universe in Chern–Simons gravity. Universe 7 (11), 428. http://dx.doi.org/10.3390/universe7110428.
Amir, M.J., Ali, S., 2015. Ricci dark energy of amended FRW universe in chern-simon modified gravity. Internat. J. Theoret. Phys. 54 (4), 1362–1369.
Amir, M.J., Ali, S., 2016. A study of holographic dark energy models in Chern–Simons modified gravity. Internat. J. Theoret. Phys. 55 (12), 5095–5105.
Bhatti, M.Z., Yousaf, Z., Nazir, M., 2023. Static cylindrically symmetric wormhole models in f(R, T) gravity. New Astron. 98. http://dx.doi.org/10.1016/j.newast.2022.101897.
Bousso, R., 2002. The holographic principle. Rev. Modern Phys. 74, 825.
Brevik, I., Timoshkin, A.V., 2021. Int. J. Geom. Methods Mod. Phys. 18, 2150149.
Caldwell, R.R., Kamionkowski, M., Weinberg, N.N., 2003. Phantom energy and cosmic doomsday. Phys. Rev. Lett. 91, 071301.
Chakraborty, G., Chattopadhyay, S., Güdekli, E., 2021a. Res. Astron. Astrophys. 21, 317.
Chakraborty, G., Chattopadhyay, S., Güdekli, E., Radinschi, I., 2021b. Thermodynamics of barrow holographic dark energy with specific cut-off. Symmetry 13, 562.
Daly, R.A., et al., 2008. Improved constraints on the acceleration history of the universe and the properties of the dark energy. Astrophys. J. 677 (1).
Granda, L.N., Oliveros, A., 2008. Infrared cut-off proposal for the holographic density. Phys. Lett. B 669 (5), 275–277.
Granda, L.N., Oliveros, A., 2009. New infrared cut-off for the holographic scalar fields models of dark energy. Phys. Lett. B 671 (2), 199–202.
Guarrera, D., Hariton, A.J., 2007. Papapetrou energy–momentum tensor for Chern–Simons modified gravity. Phys. Rev. D 76, 044011.
Guo, Z.K., Piao, Y.S., Zhang, X.M., Zhang, Y.Z., 2005. Cosmological evolution of a quintom model of dark energy. Phys. Lett. B 608, 177.
Hossienkhani, H., Azimi, N., Yousefi, H., 2021. Constraints on the Ricci dark energy cosmologies in Bianchi type I model. Int. J. Geom. Methods Mod. Phys. 18 (06), 2150095.
Huterer, D., Cooray, A., 2005. Uncorrelated estimates of dark energy evolution. Phys. Rev. D 71, 023506, arXiv:astro-ph/0404062.
Huterer, D., Turner, M.S., 2001. Probing the dark energy: Methods and strategies. Phys. Rev. D 64, 123527, arXiv:astro-ph/0012510.
Jackiw, R., Pi, S.Y., 2003. Chern–Simons modification of general relativity. Phys. Rev. D 68 (10).
Jahromi, A.S., Moosavi, S.A., Moradpour, H., Morais, J.P., Graa, I.P., Lobo, I.G., Salako, Jawad, A., 2018. Generalized entropy formalism and a new holographic dark energy model. Phys. Lett. B 780, 21.
Jawad, A., Sohail, A., 2015. Cosmological evolution of modified QCD ghost dark energy in dynamical Chern–Simons gravity. Astrophys. Space Sci. 55, 359.
Karmakar, S., Chattopadhyay, S., Radinschi, I., 2020. A holographic reconstruction scheme for f(R) gravity and the study of stability and thermodynamic consequences. New Astron. 76, 101321.
Khurshudyan, M., 2016. On a holographic dark energy model with a Nojiri–Odintsov cut-off in general relativity. Astrophys. Space Sci. 361 (12), 392.
Knop, R.A., Aldering, G., Amanullah, R., Astier, P., Blanc, G., Burns, M., Ellis, R., et al., 2003a. New constraints on wm, wl, and w from an independent set of 11 high-redshift supernovae observed with the hubble space telescope. Astrophys. J. 598 (1), 102.
Knop, R.A., et al., 2003b. New constraints on O_M, O_A, and ω from an independent set of eleven high-redshift supernovae observed with HST. Astrophys. J. 598, 102, arXiv:astro-ph/0309368.
Komatsu, E., Smith, K., Dunkley, J., Bennett, K., Gold, B., Hinshaw, G., Jarosik, N., Larson, D., Nolta, M., Page, L., et al., 2011. Seven-year wilkinson microwave anisotropy probe (WMAP) observations: cosmological interpretation. Astrophys. J. Suppl. Ser. 192 (2), 18.
Konno, K., Matsuyama, T., Asano, Y., Tanda, S., 2008. Flat rotation curves in Chern–Simons modified gravity. Phys. Rev. D 78, 024037.
Kumar, P.S., Pankaj, S., Sharma, U.K., 2022. Quintessence model of tsallis holographic dark energy. New Astron. 96, 101829. http://dx.doi.org/10.1016/j.newast.2022.101829.
Landim, R.C.G., 2016. Holographic dark energy from minimal supergravity. Internat. J. Modern Phys. D 25 (04), 1650050.
Li, M., 2004. A model of holographic dark energy. Phys. Lett. B 603, 1–5.
Li, M., Li, X.D., Wang, S., Wang, Y., 2011. Dark energy. Commun. Theor. Phys. 56, 525–604.
Linder, E.V., 2003. Exploring the expansion history of the universe. Phys. Rev. Lett. 90, 091301, arXiv:astro-ph/0208512.
Ma, Y.Z., 2008. Variable cosmological constant model: The reconstruction equations and constraints from current observational data. Nuclear Phys. B 804, 262–285.
Malik, A., Mushtaq, A., Saqib, M., 2021. Some dark energy cosmological models in $f(R,\phi)$ gravity. New Astron. 89, 101631. http://dx.doi.org/10.1016/j.newast.2021.101631.
Mamon, A.A., 2020. Study of tsallis holographic dark energy model in the framework of fractal cosmology. Modern Phys. Lett. A http://dx.doi.org/10.1142/S021773232050251X.
Martin, J., 2008. Quintessence: A mini-review. Modern Phys. Lett. A 23, 1252–1265.
Melchiorri, A., Mersini, L., Odman, C.J., Trodden, M., 2003. The state of the dark energy equation of state. Phys. Rev. D 68, 043509, arXiv:astro-ph/0211522.
Moradpour, H., Moosavi, S., Lobo, A., Morais, I.P., Jawad, A., Salako, I.G., 2018. Thermodynamic approach to holographic dark energy and the Rényi entropy. Eur. Phys. J. C 78, 829.
Nandi, K.K., Kizirgulov, I.R., Mikolaychuk, O.V., Mikolaychuk, N.P., Potapov, A.A., 2009. Quantum phase shift in Chern–Simons modified gravity. Phys. Rev. D 79, 083006.
Nojiri, S., Odintsov, S.D., 2017. Covariant generalized holographic dark energy and accelerating universe. Eur. Phys. J. C 77 (8), 528.
Nojiri, S., Odintsov, S.D., Paul, T., 2021. Different faces of generalized holographic dark energy. Symmetry 13, 928.
Nojiri, S., Odintsov, S.D., Saridakis, E.N., 2019a. Holographic inflation. Phys. Lett. B 797, 134829.
Nojiri, S., Odintsov, S.D., Saridakis, E.N., 2019b. Modified cosmology from extended entropy with varying exponent. Eur. Phys. J. C 79, 242.
Pasqua, A., da Rocha, R., Chattopadhyay, S., 2015. Holographic dark energy models and higher order generalizations in dynamical Chern–Simons modified gravity. Eur. Phys. J. C 75, 44.
Perlmutter, S., Aldering, G., Goldhaber, G., Knop, R.A., Nugent, P., Castro, P.G., Deustua, S., Fabbro, S., Goobar, A., Groom, D.E., et al., 1999. Measurements of Ω and Λ from 42 high-redshift supernovae. Astrophys. J. 517, 565–586.
Porfirio, P.J., Fonseca-Neto, J.B., Nascimento, J.R., Petrov, A.Y., 2016. On the causality aspects of the dynamical Chern–Simons modified gravity. Phys. Rev. D 94, 104057.
Riess, A.G., Filippenko, A.V., Challis, P., Clocchiatti, A., Diercks, A., Garnavich, P.M., Gilliland, R.L., Hogan, C.J., Jha, S., Kirshner, R.P., et al., 1998. Observational evidence from supernovae for an accelerating universe and a cosmological constant. Astron. J. 116, 1009.
Shaikh, A.Y., 2022. Panorama behaviors of general relativistic hydrodynamics and holographic dark energy in f(R, T) gravity. New Astron. 91, 101676.
Shekh, S.H., 2021. Models of holographic dark energy in f(Q) gravity. Phys. Dark Univ. 33, 100850.
Spergel, D.N., Verde, L., Peiris, H.V., Komatsu, E., Nolta, M., Bennett, C., Halpern, M., Hinshaw, G., Jarosik, N., Kogut, A., et al., 2003. First-year wilkinson microwave anisotropy probe (WMAP) observations: determination of cosmological parameters. Astrophys. J. Suppl. Ser. 148 (1), 175.
Susskind, L., 1995. The world as a hologram. J. Math. Phys. 36, 6377. http://dx.doi.org/10.1063/1.531249, [hep-th/9409089].
Tegmark, M., et al., 2004. The 3D power spectrum of galaxies from the SDSS. Astrophys. J. 606, 702, arXiv:astro-ph/0310725.
Telali, E.C., Saridakis, E.N., 2022. Power-law holographic dark energy and cosmology. Eur. Phys. J. C 82, 466. http://dx.doi.org/10.1140/epjc/s10052-022-10411-z.
Wang, S., Wang, Y., Li, M., 2017. Holographic dark energy. Phys. Rep. 696, 1–57.
Witten, E., 1998. Anti de sitter space and holography. Adv. Theor. Math. Phys. 2, 253.
Younas, M., Jawad, A., Qummer, S., Moradpour, H., Rani, S., 2019. Cosmological implications of the generalized entropy based holographic dark energy models in dynamical Chern–Simons modified gravity. Adv. High Energy Phys. 2019, 1287932.
Zhuravlev, V.M., 2001. Two-component cosmological models with a variable equation of state of matter and with thermal equilibrium of components. J. Exp. Theor. Phys. 93, 903–919, 1850145-19.
Zobnin, A.V., Nefedov, A.P., Shchikov, S., et al., 2000. On the charge of dust particles in a low-pressure gas discharge plasma. J. Exp. Theor. Phys. 91, 483–487.